Proceedings of ISFOG 2025
5TH INTERNATIONAL SYMPOSIUM ON
FRONTIERS IN OFFSHORE GEOTECHNICS
Nantes, France | June 9-13 2025

ISBN 978-2-85782-758-0

An investigation of the impact of drainage conditions on the interface resistance between pipelines and soils using a novel test setup

R. Houhou
American University of Beirut, Beirut, Lebanon

S. S. Najjar*, S. Sadek, and E. Shammas
American University of Beirut, Beirut, Lebanon

**sn06@aub.edu.lb (corresponding author)*

ABSTRACT: The design of offshore pipelines is governed by the axial interface resistance between the pipe and the soil. Underestimating this resistance leads to low predicted compressive forces and excessive pipeline expansion, while overestimating it can result in high compressive forces and increased lateral buckling, necessitating costly restraining structures. Therefore, reliable, cost-effective quantification of axial pipe-soil interface resistance is crucial for rational pipeline design. Uncertainty in resistance predictions arises from factors such as shearing rate, drainage conditions, consolidation periods, interface roughness, and normal stress levels. This paper investigates the efficiency and functionality of an innovative, cost-effective test setup to quantify pipe-soil interface resistance under varying drainage conditions and loading rates. Previously used to measure the drained pipe-clay interface response, this study extends its use in a laboratory setting to measure the undrained pipe-clay interface response. While the setup accurately measured drained friction factors, undrained tests proved more complex due to slight rotations in the test section affecting pore pressure readings. Despite these challenges, the undrained results were promising, demonstrating the setup's practicality and potential for further development and in-situ deployment.

Keywords: pipe-soil interaction; in-situ test; offshore pipelines

1 INTRODUCTION AND BACKGROUND

The growing demand for hydrocarbons has driven the development of deep-water offshore fields, where pipelines are essential for transporting hydrocarbons to storage facilities. The cost of these pipelines is a major component of overall project expenses, especially in deep-water settings (~3000 m) (Bai and Bai, 2005). To optimize pipeline design and minimize costs, reliable methodologies are needed to assess the soil-structure interaction (SSI) between the pipeline and surrounding soil which plays a crucial role in pipeline performance under operational loads.

Offshore pipelines experience high pressure and temperature, causing expansion and contraction that may lead to buckling or walking after repeated operational cycles (Najjar et al. 2007). The axial resistance at the pipe-soil interface counters these movements, generating compressive forces within the pipeline walls. Incorrect estimation of this resistance can lead to excessive expansion or lateral buckling, requiring costly mitigation measures.

Modelling pipeline response is complex due to changing drainage conditions at the pipeline-soil interface, which shift from undrained to drained over the pipeline's operational life (Ballard and Jewell, 2013; Boukpeti and White, 2017). The interface strength is influenced by factors such as the laying process, pore pressure dissipation, and consolidation due to the pipeline's weight. Accurate characterization of axial resistance under these conditions is essential for designing efficient pipelines.

Various testing methods, including laboratory tests (Boukpeti and White, 2017), model tests (Boylan et al., 2014), and in-situ tests (Ballard and Jewell, 2013), have been developed to estimate axial resistance. Researchers have created frameworks to capture the sensitivity of axial resistance to various testing conditions, which can help optimize pipeline design. However, reliable, cost-effective in-situ testing methods are still needed.

In-situ testing is the most reliable method for measuring axial resistance, but available equipment has limitations. The Fugro SMARTPIPE (Ballard & Jewell, 2013), for example, measures both axial and lateral pipe-soil interaction but is costly and requires specialized vessels. Other tools, such as Stanier et al.'s (2015) dragging tool and Schneider et al.'s (2020) "pipe-like" penetrometer, also have limitations in terms of precision and applicability.

This paper aims at investigating the efficiency and functionality of a first generation innovative, cost-effective and reliable test setup to quantify the pipe-soil interface resistance under different drainage conditions and loading rates. The proposed test setup has been previously utilized (Houhou et al. 2022a) to successfully measure the drained pipe-clay interface response. This study aims at utilizing the same test setup in a laboratory setting to measure the "undrained" pipe-clay interface response.

2 NOVEL TEST SETUP

The prototype is comprised of a semi-circular 1-m long half-pipe with a diameter of 160mm. The pipe section is constituted of five independent stainless-steel sheets that are folded into half-pipes of different lengths. A schematic of the apparatus prototype is presented in Figure 1. During the consolidation stage, the 5 pipe sections are connected by lateral screws to a common 1-m long aluminum bar as shown in Figure 1. The screws pass through 30-mm thick plastic spacers and connect to the aluminum bar to ensure that the 5 pipe sections act as a rigid body to apply a uniform vertical stress along the pipe length once the setup is laid on the clay surface.

At the completion of consolidation, each section takes on a specific role that was designed to facilitate the displacement-controlled shearing process: (1) The central pipe section which is 200 mm long functions as the main test section that will be displaced axially during shearing; (2) the two adjacent 50mm-long sections are dummies that will be removed prior to the test, thus creating a path that would allow for the lateral displacement of the central section without subjecting it to passive resistance on either end; (3) the 350mm pipe sections at the two ends of the pipe function as "anchoring" sections that provide the reactions needed to displace the central test section.

Prior to shearing, the screws connecting the central pipe section and the two dummies to the central aluminum bar are removed. The shearing displacement is applied via a stepper motor that is supported on the rigid aluminum bar. The motor allows for different shearing rates, thus ensuring the option of performing either drained ("very slow"), partially drained or undrained conditions ("fast"). The displacement rates range from 1.67×10^{-7} to 0.22 mm/s. During the consolidation stage, the weight of the motor (93 N) is distributed to all pipe sections and constitutes a major part of the applied normal stress. In the shearing phase, the weight of the motor shifts to the two 350-mm pipe sections at the ends. Once the central test section is detached from the aluminium bar, it will function as an independent pipe that subjects the soil beneath it to a normal stress governed by its own weight.

The motor allows for a maximum displacement of 40 mm. The screw of the motor is connected to the central test section and to an S-shape load cell using a rigid steel plate. A linear vertical displacement transducer is fixed on the aluminium bar to measure the horizontal displacement of the test section. A target and a checkerboard are fixed on the test section and the dummies/anchor sections to track the motion of the setup in different directions using a computer vision approach. Two pore pressure sensors are fitted inside the test section at two different locations to measure the induced excess pore pressures during the various testing stages (Figure 2b). The total weight of the setup when all the system components are connected is 206 N. The weight of the test section when detached from the aluminium bar is around 41 N. The actual normal stress that is acting on the pipe-soil interface ranges between 1 and 4.5 kPa depending on the final embedment of the pipe after consolidation.

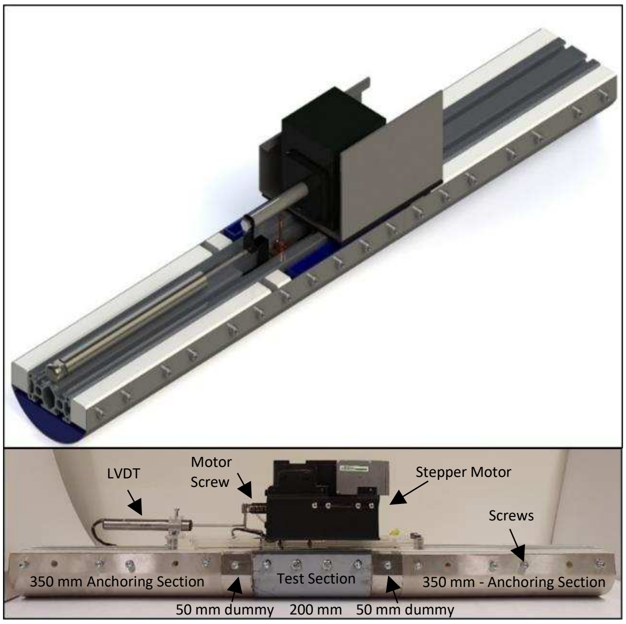

Figure 1. 3D and 2D-Frontal view of the in-situ setup

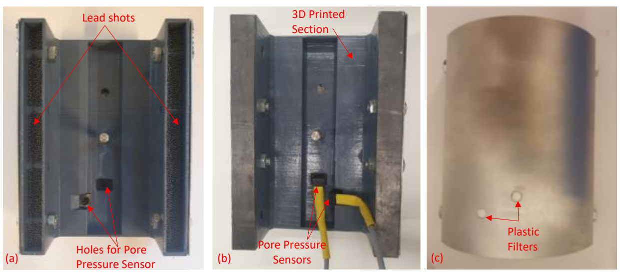

Figure 2. 3D Printed mid-section: (a, b) top view, and (c) bottom view.

3 EXPERIMENTAL PROGRAM

The soil used in the test is a natural clay constituted of 38% clay, 36% silt and 26% sand. The specific gravity of the soil is 2.64 and it is classified as a low plasticity clay (CL) according to the USCS, with a liquid limit of 29% and a plastic limit of 16.4%. One-dimensional consolidation tests indicated that its coefficient of consolidation is around C_v =1.6 m^2/year at 1.4 kPa, and the compression index and swelling index are 0.221 and 0.014, respectively.

The oven-dried soil was mixed at 40% water content which corresponds to 1.4 times its liquid limit. A 300 mm thick layer of this mix was placed in a 1.1x1.2x0.5m steel tank atop of a 100 mm gravel layer separated by a geotextile filter fabric. The consolidation process of the clay slurry was completed in three stages: (1) under the soil own weight for 10 days, (2) under a pressure of 0.7 kPa for 20 days and (3) under a pressure of 1.4 kPa for 140 days. The soil was loaded by means of steel plates to ensure a uniform pressure distribution and the drainage was permitted in the horizontal and vertical directions via geotextile sheets placed at the tank sides and between the clay and the gravel. Following the completion of the consolidation stages, water was added continuously to maintain a 2 cm water cover above the mudline and thus ensure that the clay remains saturated until the start of the tests.

Shortly before the planned implementation of the testing program, lockdowns forced an absence of students and staff from the labs and resulted in the loss of the 2 cm water cover for a period of 2 to 3 weeks. As a result, the uppermost surface of the bed showed signs of desiccation. Given the excessive time that would be needed to remold and reconsolidate the whole thickness of the clay bed (30 cm), and since the expected pipe embedment in the envisaged tests was restricted to less than 2.5cm, a decision was made to rewet, remold and reconsolidate only the upper 5cm of the bed in preparation for the resumption of the test program/schedule. As such, water was added gradually/continuously and left to wet the exposed surface for a period of 3 months. The upper 5 cm of the bed were then manually mixed/remolded in preparation for consolidation under a uniform applied pressure of 1.5 kPa. The final settlement after 45 days of consolidation was 4 mm.

Samples were taken at various locations from the upper 3 cms of the clay bed and yielded water contents of 28.5 to 30%. These water contents lead to the conclusion that the process of wetting, reconstituting, and reconsolidating the upper 5cms of the bed may not have returned the bed to a normally consolidated state. e-log p curves from reconstituted specimens and more importantly from an undisturbed specimen that was extracted from the upper 30 mm of the clay bed indicate that the measured water content of about 28% corresponds to a pressure of 10 to 12 kPa, if it were to be associated with the virgin compression line. As such, the relevant depth of the clay bed (upper 50mm) is expected to present an over-consolidated clay response in the subsequent interface tests. This is confirmed in the undrained strength profile in Fig 3a.

A pipe coating consisting of a stainless steel "smooth" surface with average surface roughness Ra, measured using a sensitive profilometer of 0.08 µm was used in the testing program. Figure 3b presents a scanning electron microscope image that reveals the roughness of the stainless steel relative to the tested clay at a scale of about 50 microns. The figure clearly illustrates the contrast between the roughness of the stainless steel and the clay and captures the presence of "large" sand particles in the tested clay. The stainless steel is thus considered as a smooth interface.

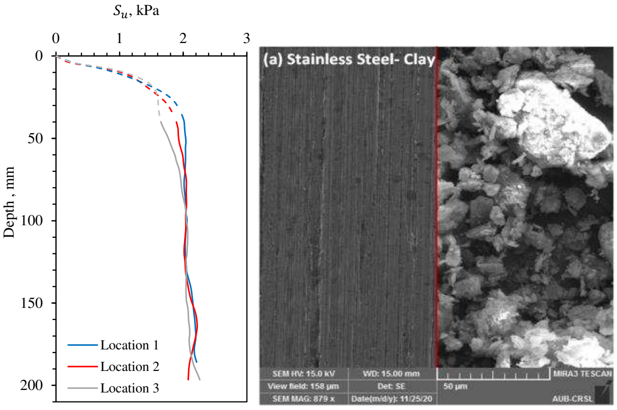

Figure 3. (a) Undrained strength from a ball penetrometer and (b) contrast between stainless steel and tested clay.

4 TEST RESULTS

In a first series of tests, the 1-m pipe section was placed on the clay bed and left to consolidate under its own weight until primary consolidation was completed (2 days). The dummy sections were then removed, and the middle section detached from the aluminum bar and left for half an hour for the pore pressures to stabilize. A total of 22 sweeps (30-35 mm of displacement) with a change of direction between successive sweeps were performed, while varying the shearing rate (undrained versus drained tests) and the pause periods prior to shearing. Test results include the response of the pipe section during the penetration and consolidation stages and during axial shearing.

Figure 4 shows the pore pressure measurements during the pipe laying process and the following dissipation of the pore pressures generated and resulting consolidation. Upon "touchdown", the setup generated an immediate settlement of 4.4 mm in less than 15 seconds. As the pipe embedment reached and exceeded 3 mm, the pore pressure sensor at 20 degrees became in contact with the soil and recorded an increase in pore water pressure. During the post-laydown consolidation, the generated excess pore pressures dissipated, and the pipe settlement increased by about 0.5 mm over a time period of about 8 hours (Figure 4). The final pipe embedment of 5 mm indicates that the effective normal stress at the clay/pipe interface is about 3.7 kPa including wedging effects. Figure 5 shows the setup with the camera used to detect/record the patterns fixed on the setup.

The first shearing sequence (F1) consisted of 4 shearing cycles (8 sweeps) that were conducted at a fast shearing rate (0.2 mm/s). Results are presented in Figure 6 and show the mobilization of the interface shear stress and generation of excess pore pressure at the side and invert of the test section. Results indicate that the mobilized interface shear stresses during “undrained” shear exhibited a peak at relatively small pipe displacements (0.1 to 0.2mm). Following the peak, an abrupt reduction in stresses was observed leading to minimum observed shear stresses at displacements in the order of 0.3mm. The interface response in the first cycle was unique compared to the remaining 3 cycles in the sense that the pipe mobilized a significant proportion of the clay’s undrained shear strength, with a maximum interface resistance of 1.4 kPa (compared to a clay/clay undrained strength of about 2.0 kPa). This relatively high interface resistance is almost twice that observed in the loading cycles that followed (maximum stress ranging from 0.7 to 0.85 kPa), indicating that clay remolding must have occurred at the interface in subsequent cycles.

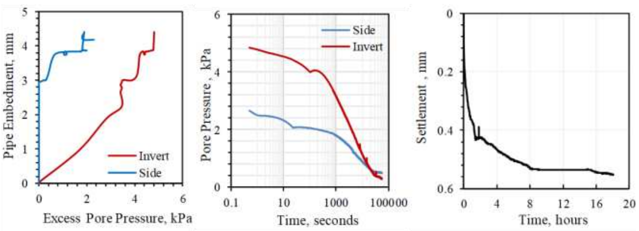

Figure 4. (a) Pore pressure measurements during pipe laying process, (b) dissipation of pore pressure post-lay, and (c) consolidation post lay.

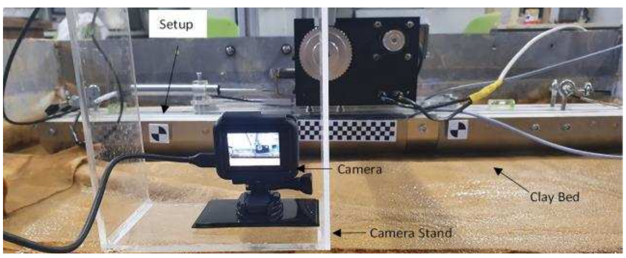

Figure 5. Setup after consolidation

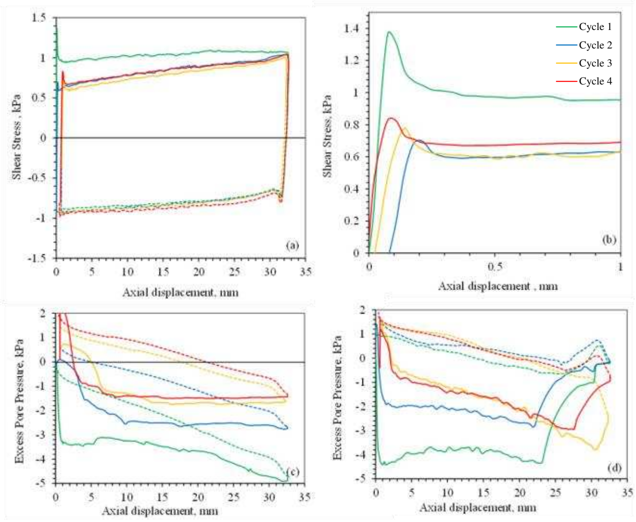

Figure 6. The axial response during F1-S1: (a, b) shear-stress variation, (c, d) excess pore pressures at the pipe invert and side.

The second observation is that the mobilized interface shear stresses increased from a displacement of 1mm to the maximum displacement (~ 33mm). This increase in interface strength with axial displacement could be attributed to multiple factors that are related to the generation of negative pore pressures and their dissipation or to passive resistance at the front of the pipe section due to a thin layer of clay that could have been dragged during shear (Figure 7). In the reversal sweep that followed the first sweep, a significant reduction in the maximum shear stress occurred (~ 0.7 kPa compared to 1.4 kPa in the first sweep). During the three following cycles, the shear stresses dropped after the peak to almost the same minimum interface shear stress of 0.65 kPa (Figure 6b). The reduction observed in the undrained interface shear resistance after the first cycle could be attributed to remolding of the clay under the pipe section and possible alignment of the clay particles at the clay/pipe interface. The consistent shear stress versus displacement response that was observed in cycles 2 to 4 is a testimony of the ability of the novel test setup to produce results with a high level of repeatability, which is a very important metric in the assessment and evaluation of new testing systems in geotechnical engineering.

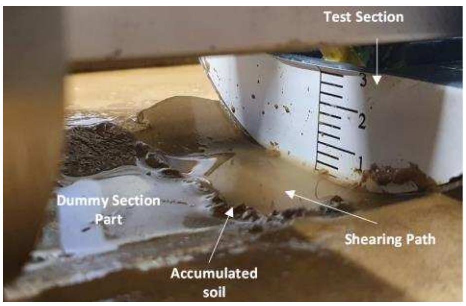

Figure 7. Close up view of the shearing zone

The excess pore pressure generated during shearing cycles is presented as a function of pipe displacement in Figure 6c. Results indicate that shearing at the pipe/clay interface generated negative pore pressures at the pipe invert and side during the first sweep of each cycle. These negative pore pressures confirm the over consolidated state of the clay at the clay/pipe interface. The magnitude of the negative pore pressure reduced with shearing cycles as a result of the cumulative shearing strains and associated remolding of the clay under the pipe. Moreover, results indicate that the negative pore pressure that were generated in the first sweep of every cycle dissipated gradually during the reversal sweep of that cycle. Interestingly, pore pressures measured on the side of the pipe indicated that dissipation of negative pore pressure started in the middle of the sweep (Figure 6d) despite the relatively fast shearing rate applied (0.2 mm/sec). Such dissipation of pore water pressure was not observed at the pore pressure sensor located at the invert and is thus related to the shorter drainage path, given that the location of the sensor is closer to the clay surface. The shorter drainage path allowed for partial dissipation of pore pressures during shearing.

Caution should be exercised before drawing conclusions about the pore pressure response along the full length of the clay/pipe interface. The complexity observed in the non-uniform generation of excess pore water pressure along the pipe section and its possible dissipation during the different cycles and sweeps, coupled with the limited number of pore pressure sensor used, prohibit any in-depth analysis of the pore pressure response. Consequently, the results presented in Figure 6 should only be considered to be indicative of the local pore pressure response.

For the purpose of completing the undrained interface tests, three additional cycles of loading (F2, F3, and F4) were conducted, with a waiting time of 24 hours between cycles. The objective was to investigate whether the undrained interface response will exhibit any hardening or softening as a result of repeated cycles, with enough waiting time allowed for the dissipation of pore water pressure and full consolidation between cycles.

Results of undrained cycles F2, F3, and F4 are presented in Figure 8. They indicate that the shear response and the excess pore pressure generation were approximately the same for all cycles. This observation shows that the undrained interface resistance for the over consolidated clay tested in this study did not exhibit strain hardening between repetitive loading cycles, despite the waiting time that was enforced. These results are expected since improvements in the undrained interface response as a result of repeated cycles with a waiting time have only been reported for normally consolidated soft clay in the published literature (Smith and White, 2014). For the over consolidated clay tested in this study, the absence of softening in the interface response with repeated cycles is anticipated, particularly for the case of a smooth stainless steel interface where the failure/slip zone in which the shear strains are concentrated is relatively thin.

Interestingly, the maximum observed interface shear stresses in F2, F3, and F4 (~ 1.2 kPa) exceeded the stresses measured in the last cycle of F1 (~ 0.82 kPa), indicating that the clay under the pipe benefited from the 24 hour waiting period. For test F3, an additional cycle was conducted immediately after the first cycle (no waiting time) to investigate whether a reduction in interface shear resistance may be observed. As expected, results on Figure 8 indicate that consecutive shearing cycles with no waiting time in F3 lead to a clear reduction in the measured interface shear stresses.

Following the 16 undrained sweeps in cycles F1 to F4, the drained interface clay/steel response was measured in tests D1 (shear rate ~ 0.00062 mm/s) and D2 (shear rate ~ 0. 00032 mm/s). Results of the drained tests are presented in Figure 9. The tests exhibited an identical interface shear stress versus displacement response with negligible generation of excess pore pressure during shearing. The shear stress reached a peak of about 1.15 kPa after about 0.4 mm of displacement which falls in the range of 0.3% to 0.8% of the pipe diameter as reported by Dendani et al. (2007). The peak stress corresponds to a drained friction coefficient of about 0.31 and a secant interface friction angle of 17.5°. After the peak, the shear stress decayed rapidly to a minimum value of 0.97 kPa (friction angle of 15.2°) and remained more or less constant over the 25 mm of pipe displacement.

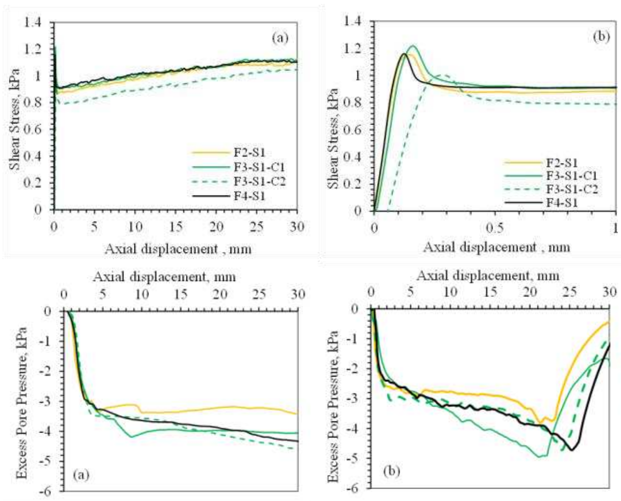

Figure 8. Shear and Pore pressures during F2, F3, and F4 at: (a) invert and (b) side of the test section.

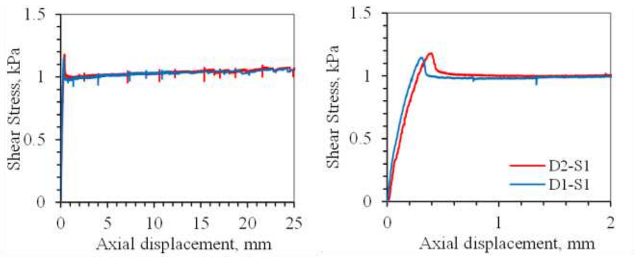

Figure 9. Drained clay/steel interface response

5 CONCLUSIONS

Proof of concept tests of a proposed in-situ setup highlighted its potential in accurately estimating the pipe-soil interface response under undrained and drained loading. The setup was tested under different testing conditions inside a soft clay bed and resulted in the following conclusions:

1. The smooth interface response was perfectly captured by the novel in-situ setup during drained and undrained shearing. Based on the testing conditions, the peak and the residual resistances were successfully measured.
2. Under undrained conditions, the measured interface response was realistic, despite the fact that the test section exhibited slight uncontrolled rotations when it was pushed fast. For the case of slow drained tests, the rotations were smaller and the movement was more controlled.
3. The drained interface resistance could be reliably and repeatedly measured. The resulting secant friction angles and residual drained friction factors compare favourably with the results of the direct shear tests performed on the same soil and the same interfaces (see Houhou et al. 2022b).
4. The pore pressures measurement were repeatable during both loading and consolidation steps, which gives the test setup an added value when it comes to understanding performance.

Future work will test the setup using pipe sections having a variety of surface roughness values and under different scenarios of embedment depths.

AUTHOR CONTRIBUTION STATEMENT

Roba Houhou: Experimental Testing, Data Analysis, Writing of Paper Draft. **Shadi Najjar and Salah Sadek**: Methodology, Interpretation of Test Results, Supervision, and Editing Paper. **Elie Shammas**: Support in Design, Fabrication, and Installation of Sensors and Mechanical Systems

ACKNOWLEDGEMENTS

The authors would like to acknowledge the Munib and Angela Masri Institute of Energy and Natural Resources and the University Research Board at the American University of Beirut for funding this research.

REFERENCES

Bai, Y. and Bai, Q. (2005). *Subsea Pipelines and Risers*, Amsterdam, the Netherlands, Elsevier

Ballard, J.C. and Jewell, R. (2013). Observations of Pipe-Soil Response from In-Situ Measurements. In *Offshore Technology Conference*, OTC-24154-MS, Houston, TX.

Boukpeti, N. and White, D. J. (2017). Interface Shear Box Tests for Assessing Axial Pipe–Soil Resistance. *Géotechnique* 67(1): 18–30. https://doi.org/10.1680/jgeot.15.P.112

Boylan, N., White, D.J. and Brunning, P. (2014). Seabed Friction on Carbonate Soils: Physical Modelling of Axial Pipe-Soil Interaction. In *Offshore Technology Conference*, OTC-25398-MS, Houston, TX.

Houhou, R., Sadek, S., Najjar, S. and Shammas, E. (2022). A Novel Proof of Concept Experimental Setup for Seabed-Pipe Interface Friction Measurements. *Geotechnical Testing Journal* 45(5): 915–935. https://doi.org/10.1520/GTJ20210192.

Houhou, R., Bou Mjahed, R., Sadek, S., and Najjar, S. (2022). Drained Axial Pipe-Soil Resistance at Low Confinement Using Tilt Table and Direct Shear Tests. *Journal of Geotechnical and Geoenvironmental Engineering*, 148(11): 04022086.

Najjar, S., Gilbert, R.B., Liedtke, E., McCarron, B. and Young, A. G. (2007). Residual Shear Strength for Interfaces between Pipelines and Clays at Low Effective Normal Stresses. *Journal of Geotechnical and Geoenvironmental Engineering* 133(6): 695–706. https://doi.org/10.1061/(ASCE)1090-0241(2007)133:6(695)

Schneider, M.A., Stanier, S.A., White, D.J. and Randolph, M.F. (2020). Apparatus for Measuring Pipe-Soil Interaction Behavior Using Shallow 'Pipe-Like' Penetrometers. *Geotechnical Testing Journal* 43(3): 622–640. https://doi.org/10.1520/GTJ20180293

Stanier, S.A., White, D.J., Chatterjee, S., Brunning, P. and Randolph, M.F. (2015). A Tool for ROV-Based Seabed Friction Measurement. *Applied Ocean Research* 50: 155–162. https://doi.org/10.1016/j.apor.2015.01.016